The Dark Side of the Cosmos:

Exploring Dark Energy and Modified Gravity

RENATA meeting 2025 (Zaragoza, Spain)

Mariam Bouhmadi-López

IKERBASQUE & EHU (Spain)

September 22nd, 2025

Table of contents

Introduction

Introduction-1-: A brief sketch of the universe

- The universe is homogeneous and isotropic on large scales (cosmological principle)
- The matter content of the universe:
  - Standard matter
  - Dark matter
  - Something that induce the late-time acceleration of the Universe
- The acceleration of the universe is backed by several measurments: $H(z)$, SneIa, BAO, CMB, LSS (matter power spectrum, growth function)...

Introduction-2-

- Such an acceleration could be due to:
  - A new component of the energy budget of the universe: dark energy; i.e. it could be Λ (i.e. a non dynamical dark energy), quintessence, of a phantom(-like/effective) nature
  - A change on the behaviour of gravity on the largest scale. No new component on the budget of the universe but rather simply gravity modifies its behaviour, within a metric, Palatini (affine metric), in presence of torsion or non-metricity ....

Cosmological problems

- If Λ is driving the current acceleration of the Universe, then:
    - Coincidence problem. How is this sensible to initial conditions?
    - Why now? Dark energy seems to be dominant only at late-time, not before.
    - Fine-tuning problem. New energetic scale $\rho_\Lambda \approx 10^{-47}\,\text{GeV}^4$. It is very small compared to other scales.
    - Cosmological tensions, in particular the Hubble tension.
- How might evolving dark energy models or extended theories of gravity help to address the issues discussed above?

E. Di Valentino et al. [arXiv:2504.01669 [astro-ph.CO]]

Quintessence through a genealised axion-like potential

Quintessence

- Minimally coupled canonical scalar field:

$$L = \frac{1}{2k^2}R - \frac{1}{2}g^{\mu\nu}\nabla_\mu\phi\nabla_\nu\phi - V(\phi) + L_{r,m}.$$

  - ϕ is a dynamical field.
  - **Coincidence problem.** It can be alleviated by scaling solutions and tracker fields.
  - Fine-tuning problem remains unsolved.
  - Some quintessence models allow for a natural explanation of why now?
  - Could the tensions H_0 and S_8 been alleviated?
- An axion-like potential: $V(\phi) = \Lambda^4[1 - \cos(\phi/\eta)]^{-n}$ with a generalisation to negative exponents, i.e. $0 < n$.
- Previously analised on the context of wave dark matter and early dark energy *Wave Dark Matter* (L. Hui). [arXiv:2101.11735], *Dark energy from the string axiverse* (M. Kamionkowski). [arXiv:1409.0549]

This part of the pat of the talk is based on C.G. Boiza, M.B.-L, H.-W. Chiang, 2409.18184 (EPJC), 2410.22467 (Phys. Dark Univ), 2503.04898 (JCAP) ,

Dynamical system and fixed points

- Dynamical variables (FLRW filled by rad., mat. and an axion-like field):

$$x = \frac{k\dot{\phi}}{\sqrt{6}H}, \quad y = \frac{k\sqrt{V}}{\sqrt{3}H}, \quad \lambda = -\frac{V_{,\phi}}{kV}, \quad \Gamma = \frac{V_{,\phi\phi}V}{(V_{,\phi})^2}, \quad z = \Omega_r^{1/2} = \frac{k\sqrt{\rho_r}}{\sqrt{3}H}$$

Point	x	y	z	λ	w_{eff}	Stability
A_1	0	0	0	Any	0	Saddle
A_2	0	0	1	Any	$1/3$	Saddle
E	0	1	0	0	-1	(Un)Stable if $n > 0$ ($n < 0$)

Axion-like potential

$$V(\phi) = \Lambda^4[1-\cos(\phi/\eta)]^{-n}.$$

Generalisation to $n > 0$

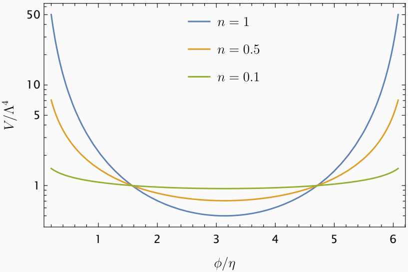

$$\lambda(\phi) = \frac{n}{k\eta}\frac{\sin(\phi/\eta)}{1-\cos(\phi/\eta)}$$

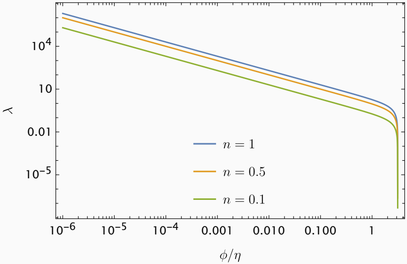

- Cosmological constant in the limit $n \to 0$.
- Minimum at $\phi/\eta = \pi \to V \approx V_{\rm min} + \frac{1}{2}m^2(\phi - \pi\eta)^2$ where $V_{\rm min} \equiv \Lambda^4/2^n$ and $m^2 \equiv n\Lambda^4/(2^{n+1}\eta^2)$.
- $\phi_{ini}/\eta \ll 1$ in order to have non-trivial evolution $\to \lambda_{ini} \gg 1$.
- **Tracking with $\omega_\phi < \omega$: $\Gamma > 1$ and $\Gamma \approx const.$ in the regime $\lambda \gg 1$.**

Fixed points and tracking

- Fixed points: A_1, A_2 and E (minimum of the potential). E is an attractor $\rightarrow$ **Late-time acceleration.**
- $\Gamma(\lambda) = 1 + \frac{1}{2n} + \frac{n}{2k^2\eta^2\lambda^2}$. In the regime $\lambda \gg 1$: $\Gamma \approx 1 + \frac{1}{2n} \rightarrow$ **Tracking behaviour** with $\omega_\phi < \omega$.
- Tracking regime given by $\omega_\phi \approx -\frac{2(\Gamma-1)}{1+2(\Gamma-1)} = -\frac{1}{1+n} \quad (\omega = 0)$.

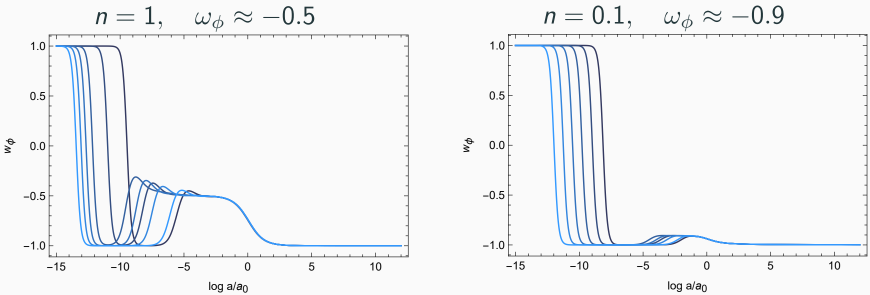

Matter power spectrum

Matter power spectrum suppression:

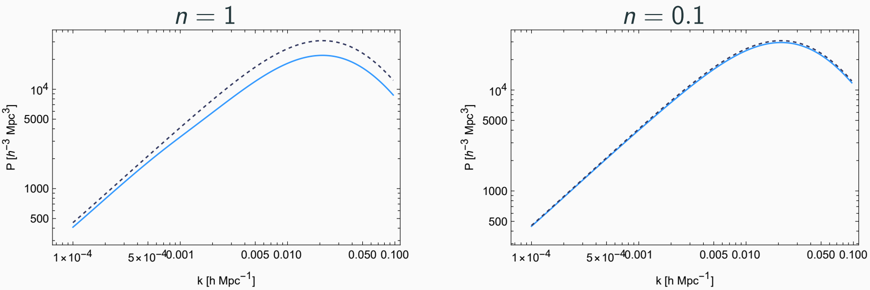

fσ8 behaviour

fσ8 distribution:

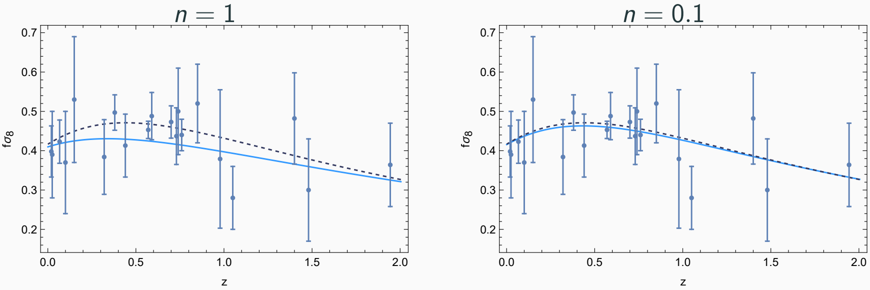

Fitting the model-1-

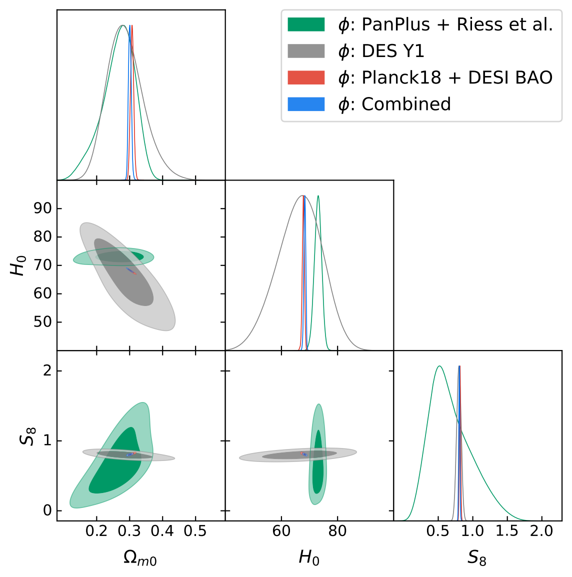

H.-W. Chiang, C.G. Boiza and M.B.-L.: arxiv:2503.04898 (JCAP)

Comparing the model

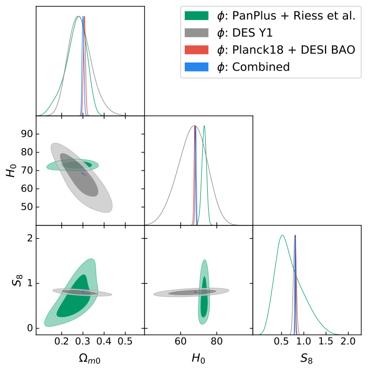

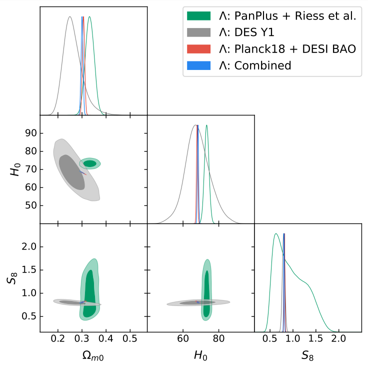

Fitting the model-2-

	CMB	+ BAO	+ SNe	+ low-z	+ DES Y1
$10^3\Omega_{b0}h^2$	22.19 ± 0.13	22.29 ± 0.12	22.26 ± 0.12	22.34 ± 0.12	22.38 ± 0.12
$10^3\Omega_{c0}h^2$	119.7 ± 1.0	118.26 ± 0.81	118.56 ± 0.79	117.80 ± 0.76	117.27 ± 0.72
$10^5\theta_{MC}$	1040.77 ± 0.25	1040.94 ± 0.24	1040.91 ± 0.24	1041.01 ± 0.24	1041.05 ± 0.24
$\ln(10^{10}A_s)$	3.037 ± 0.014	3.044 ± 0.014	3.043 ± 0.014	3.047 ± 0.014	3.046 ± 0.014
n_s	0.9636 ± 0.0040	0.9672 ± 0.0036	0.9665 ± 0.0036	0.9685 ± 0.0036	0.9693 ± 0.0036
τ_{reio}	0.0524 ± 0.0071	0.0571 ± 0.0071	0.0562 ± 0.0070	0.0587 ± 0.0071	0.0589 ± 0.0071
H_0	67.24 ± 0.46	67.89 ± 0.36	67.76 ± 0.35	68.12 ± 0.34	68.36 ± 0.32
Ω_{m0}	0.3154 ± 0.0064	0.3064 ± 0.0048	0.3082 ± 0.0047	0.3034 ± 0.0044	0.3003 ± 0.0042
σ_8	0.8077 ± 0.0055	0.8064 ± 0.0056	0.8067 ± 0.0056	0.8061 ± 0.0057	0.8041 ± 0.0055
S_8	0.828 ± 0.011	0.8149 ± 0.0090	0.8176 ± 0.0090	0.8107 ± 0.0087	0.8044 ± 0.0080
DIC	5497.90 ± 0.12	5507.21 ± 0.37	6209.34 ± 0.14	6217.77 ± 0.43	6477.38 ± 0.28
WAIC	5499.09 ± 0.50	5507.85 ± 0.18	6210.36 ± 0.21	6218.68 ± 0.21	6481.16 ± 0.22
$-\ln B$	5499.3 ± 1.1	5508.13 ± 0.73	6210.51 ± 0.44	6219.1 ± 1.4	6479.9 ± 1.2

Table 2. Mean and standard deviation of cosmological parameters, late-time observables, and statistical probes for ΛCDM model. From left to right are gradually larger datasets that progressively add in datasets of CMB, BAO, etc., as defined in section 3.1.

	CMB	+ BAO	+ SNe	+ low-z	+ DES Y1
$10^3\Omega_{b0}h^2$	22.18 ± 0.13	22.28 ± 0.12	22.28 ± 0.12	22.34 ± 0.12	22.39 ± 0.12
$10^3\Omega_{c0}h^2$	119.8 ± 1.1	118.29 ± 0.80	118.40 ± 0.83	117.73 ± 0.79	117.22 ± 0.73
$10^5\theta_{MC}$	1040.76 ± 0.25	1040.95 ± 0.24	1040.93 ± 0.24	1041.03 ± 0.23	1041.06 ± 0.26
$\ln(10^{10}A_s)$	3.039 ± 0.014	3.044 ± 0.014	3.044 ± 0.014	3.048 ± 0.014	3.048 ± 0.014
n_s	0.9634 ± 0.0040	0.9671 ± 0.0036	0.9669 ± 0.0037	0.9686 ± 0.0036	0.9694 ± 0.0035
τ_{reio}	0.0532 ± 0.0071	0.0568 ± 0.0073	0.0566 ± 0.0071	0.0590 ± 0.0072	0.0596 ± 0.0073
$\log_{10}(\rho_{DE,0}/V_{min} - 1)$	$-2.9^{+2.1}_{-0.7}$	$-2.92^{+0.45}_{-0.75}$	$-3.0^{+2.6}_{-0.6}$	$-2.94^{+0.43}_{-0.76}$	$-3.0^{+3.1}_{-0.8}$
$\log_{10}(\eta/M_P)$	$-1.25^{+0.31}$	$-2.0^{+0.8}$	-0.8	$-2.0^{+0.7}$	-0.8
n	$0^{+0.6}$	$0^{+0.6}$	$0^{+0.5}$	$0^{+0.6}$	$0^{+0.6}$
$\log_{10}(\phi_i/\eta)$	$0.5_{-3.3}$	$0.5_{-3.0}$	$0.5_{-2.0}$	$0.5_{-2.9}$	$0.5_{-1.5}$
H_0	$67.05^{+0.62}_{-0.77}$	67.77 ± 0.39	67.62 ± 0.45	68.08 ± 0.36	68.31 ± 0.33
Ω_{m0}	$0.3177^{+0.0095}_{-0.0078}$	0.3075 ± 0.0049	0.3091 ± 0.0053	0.3036 ± 0.0046	0.3006 ± 0.0042
σ_8	$0.8056^{+0.0070}_{-0.0079}$	0.8049 ± 0.0062	0.8042 ± 0.0067	0.8052 ± 0.0059	0.8035 ± 0.0059
S_8	0.831 ± 0.012	0.8149 ± 0.0091	0.8163 ± 0.0090	0.8100 ± 0.0089	0.8042 ± 0.0080
DIC	5498.13 ± 0.54	5507.87 ± 0.13	6210.08 ± 0.35	6218.58 ± 0.01	6478.21 ± 0.53
WAIC	5499.03 ± 0.53	5508.42 ± 0.15	6210.85 ± 0.03	6219.12 ± 0.29	6481.97 ± 0.92
$-\ln B$	5499.74 ± 0.99	5509.2 ± 2.4	6210.17 ± 0.04	6219.09 ± 0.20	6482.8 ± 2.8
ΔDIC	0.23 ± 0.59	0.66 ± 0.41	0.74 ± 0.39	0.81 ± 0.51	0.83 ± 0.63
ΔWAIC	-0.06 ± 0.77	0.56 ± 0.24	0.48 ± 0.45	0.43 ± 0.39	0.81 ± 0.97
$-\Delta \ln B$	0.4 ± 1.6	1.0 ± 2.4	-0.35 ± 0.52	-0.1 ± 1.7	2.9 ± 3.2

Table 3. Mean and standard deviation of cosmological parameters, late-time observables, and statistical probes for the axion-like dark energy model in section 2. From left to right are gradually larger datasets of CMB, CMB + BAO, CMB + BAO + SNe, etc., as defined in section 3.1. ΔICs are with respect to ΛCDM model presented in table 2. For parameters not following Gaussian distribution we provide the median and 68% lower and upper bounds (if valid) instead, with color coding for how heavy the tail is (red for short tail, black for Gaussian, blue for exponential, and cyan for long tail.)

Fitting the model-3-

	BAO	SNe + low-z	DES Y1
$10^3\Omega_{c0}h^2$	111 ± 11	116 ± 29	107^{+15}_{-19}
$10^5\theta_{\rm MC}$	1036 ± 12	1081^{+15}_{-18}	1048^{+36}_{-38}
$\ln(10^{10}A_s)$			$3.47^{+0.27}_{-0.29}$
$\log(\rho_{\rm DE,0}/V_{\rm min} - 1)$	$-2.8^{+2.1}_{-0.6}$	$-0.08^{+0.80}_{-0.95}$	$-1.0^{+1.8}_{-1.6}$
$\log(\eta/M_P)$	$-0.89^{+0.56}$	$0.5_{-1.0}$	$-0.3_{-1.0}$
n	0.4	$0^{+0.5}$	0.4
$\log(\phi_i/\eta)$	$0.5_{-3.2}$	-1.4	$0.5_{-2.9}$
H_0	$68.5^{+1.0}_{-1.4}$	73.0 ± 1.3	70.4 ± 5.5
Ω_{m0}	0.291 ± 0.016	$0.281^{+0.043}_{-0.053}$	0.266 ± 0.046
σ_8			0.862 ± 0.093
S_8			0.802 ± 0.031
DIC	8.53 ± 0.12	703.54 ± 0.33	260.86 ± 0.72
WAIC	8.26 ± 0.21	703.40 ± 0.45	262.36 ± 0.68
$-\ln B$	8.33 ± 0.26	703.56 ± 0.11	262.26 ± 0.29
ΔDIC	0.08 ± 0.14	0.17 ± 0.34	0.2 ± 1.1
ΔWAIC	-0.24 ± 0.27	0.09 ± 0.46	-0.27 ± 0.69
$-\Delta\ln B$	-0.53 ± 0.48	0.07 ± 0.17	-0.10 ± 0.98
Tension against	CMB	CMB + BAO	CMB + BAO + SNe + low-z
R	1.2 ± 2.8	6.3 ± 2.8	1.5 ± 2.8
GoF	$2.33 \pm 0.25\sigma$	$4.20 \pm 0.23\sigma$	$2.93 \pm 0.35\sigma$
S	$2.08 \pm 0.41\sigma$	$3.96 \pm 0.26\sigma$	$1.86 \pm 0.47\sigma$
ΔR	1.2 ± 3.1	-1.2 ± 3.2	3.1 ± 3.5
ΔGoF	$0.39 \pm 0.39\sigma$	$-0.10 \pm 0.30\sigma$	$0.39 \pm 0.46\sigma$
ΔS	$0.40 \pm 0.45\sigma$	$-0.10 \pm 0.31\sigma$	$0.26 \pm 0.48\sigma$

Table 6. Mean and standard deviation of cosmological parameters, late-time observables, and statistical probes for the axion-like dark energy model in section 2. From left to right are datasets of BAO, SNe + low-z, and DES Y1. ΔICs and delta of tension probes are with respect to ΛCDM model presented in table 5. Tension probes of $-\ln R$, GoF and S are with respect to axion-like dark energy model inside table 4 according to "Tension against" row. For parameters not following Gaussian distribution we provide the median and 68% lower and upper bounds (if valid) instead, with colour coding for how heavy the tail is (red for short tail, black for Gaussian, blue for exponential, and cyan for long tail.) If the distribution is clearly single-sided we report the modal and the single-sided 68% bound instead.

H.-W. Chiang, C.G. Boiza and M.B.-L.: arxiv:2503.04898

Observables-1-

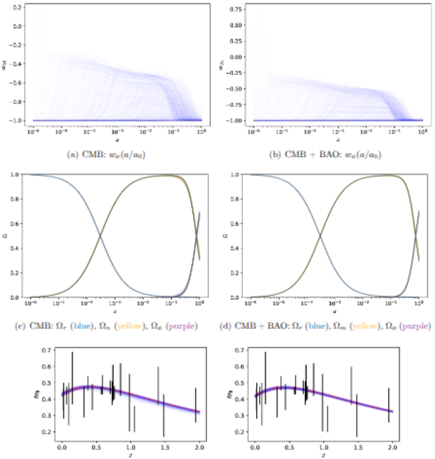

(a) CMB: $w_\phi(a/a_0)$ (b) CMB + BAO: $w_\phi(a/a_0)$

(c) CMB: Ω_r (blue), Ω_m (yellow), Ω_ϕ (purple) (d) CMB + BAO: Ω_r (blue), Ω_m (yellow), Ω_ϕ (purple)

(e) CMB: $f\sigma_8$ (f) CMB + BAO: $f\sigma_8$

Figure 8. The dark energy equation of state w_ϕ (*top*), density parameters (*centre*) of radiation Ω_r (blue), matter Ω_m (yellow) and dark energy Ω_ϕ (purple) as functions of a/a_0, and $f\sigma_8$ (*bottom*) as functions of z for 600 samples drawn from individual fits. *Left* figures: Models fitted against CMB dataset. *Right* figures: Models fitted against CMB + BAO dataset. *Black* line denotes ΛCDM model and non-black lines denote the axion-like dark energy model. Without additional distance measurement, CMB dataset alone permits variation of the density parameter evolution as depicted in Fig. 2. However, once BAO dataset is included, the density parameters stabilise and the tracking regime has to end before $a/a_0 = 1$. In *bottom* figures, the $f\sigma_8$ data are taken from table 2 of [76].

Late-time acceleration through a 3-form field

Can we have something beyond scalar fields to describe DE?

- Can we have something beyond scalar fields to describe DE?
  - A possibility come in the form of 3-forms.
  - Inspired in supergravity and string theory: Aurilia, Nicolai, Townsend (1980), Copeland, Lahiri,Wands (1995)
  - Massless 3-form as Cosmological Constant (solving CC problem): Turok, Hawking (1998)
  - Inflation or late time acceleration driven by self-interacting 3-forms: Koivisto, Nunes (2009) and (2010)
  - Non-Gaussianity: Kumar, Mulryne, Nunes, Marto, Moniz (2016)
  - Quantum cosmology with 3-forms: Bouhmadi-López, Brizuela, Garay (2018)
  - DE models (quintessence like and phantom as well): Morais, Bouhmadi-López, Kumar, Marto, Tavakoli, Phys. Dark Univ., arXiv: 1608.01679 , Bouhmadi-López, Marto, Morais and Silva, JCAP, arXiv: 1611.03100 M.B.-L, H.-W. Chiang, C.G. Boiza and P. Chen: work in progress (the observational fit)

The 3-form action

- We will consider the following action for a massive 3-form, $A_{\mu\nu\rho}$, minimally coupled to gravity

$$S^A = \int \mathrm{d}^4\mathbf{x}\sqrt{|\det g_{\mu\nu}|}\left[-\frac{1}{48}F^{\mu\nu\rho\sigma}F_{\mu\nu\rho\sigma} - V\left(A^{\mu\nu\rho}A_{\mu\nu\rho}\right)\right].$$

- The strength tensor, a 4-form, is defined through the exterior derivative: $F_{\mu\nu\rho\sigma} \equiv 4\nabla_{[\mu}A_{\nu\rho\sigma]}$
- The equation of motion, obtained from variation of S^A, is

$$\nabla_\sigma F^\sigma{}_{\mu\nu\rho} - 12\frac{\partial V}{\partial\left(A^2\right)}A_{\mu\nu\rho} = 0$$

- $\Rightarrow$ a massless 3-form is equivalent to a cosmological constanst

C. Germani and A. Kehagias, J. Cosmol. Astropart. Phys. 2009, 28 (2009)
T. S. Koivisto, D. F. Mota, and C. Pitrou, J. High Energy Phys. 2009, 92 (2009)
M. Duff and P. Van Nieuwenhuizen, Phys. Lett. B 94, 179 (1980)

3-form Cosmology

We consider a homogeneous and isotropic universe described by the Friedmann-Lemaître-Robertson-Walker line element

$$ds^2 = -dt^2 + a^2(t)\gamma_{ij}dx^i dx^j \,.$$

t - cosmic time, $\dot{\{\}} = d\{\}/dt$
a - scale factor
x^i - comoving spatial coordinates (roman indices run from 1 to 3).

Only the purely spatial components of the 3-form are dynamical:

$$A_{0ij} = 0\,, \qquad A_{ijk} = a^3(t)\chi(t)\epsilon_{ijk}\,.$$

T. S. Koivisto, D. F. Mota, and C. Pitrou, J. High Energy Phys. 2009, 92 (2009)
Koivisto and Nunes PLB [arXiv:0907.3883], idem PRD [arXiv:0908.0920]

3-form Cosmology: background equations

$\Rightarrow$ Friedmann Equation

$$3H^2 = \kappa^2 \rho_\chi = \kappa^2 \left[\frac{1}{2} \left(\dot{\chi} + 3H\chi \right)^2 + V(\chi^2) \right] .$$

$\Rightarrow$ Raychaudhuri equation

$$\dot{H} = -\frac{\kappa^2}{2} \left(\rho_\chi + P_\chi \right) = -\frac{\kappa^2}{2} \chi \frac{\partial V}{\partial \chi} .$$

A 3-form can show phantom-like behavior if $\partial V / \partial \chi^2 < 0$.

$\Rightarrow$ Equation of motion

$$\ddot{\chi} + 3H\dot{\chi} + 3\dot{H}\chi + \frac{\partial V}{\partial \chi} = \ddot{\chi} + 3H\dot{\chi} + \left(1 - \frac{\chi^2}{\chi_c^2} \right) \frac{\partial V}{\partial \chi} = 0 .$$

3-form Cosmology: evolution of χ

- Independently of the shape of a regular potential, in absence of DM interaction, the 3-form decays rapidly towards the interval $[-\chi_c, \chi_c]$ Koivisto and Nunes PLB [arXiv:0907.3883], idem PRD [arXiv:0908.0920]

- In an expanding Universe, once inside the interval $[-\chi_c, \chi_c]$, the 3-form will end up in one of the minima of the potential (notice $V_{\rm eff} \neq V$).

- If the 3-form stops at the limits of this interval:

$$\chi = \pm\chi_c \quad \text{and} \quad \dot{\chi} = 0$$

- $\longrightarrow$ Universe heads towards a LSBR event $(\chi_c = \sqrt{2/3\kappa^2})$

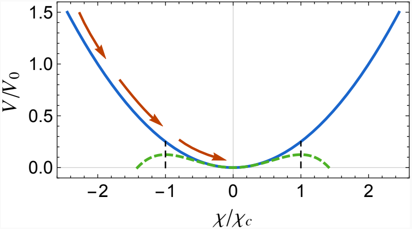

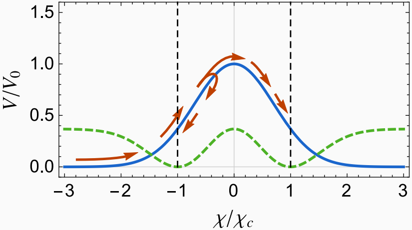

3-forms & with a Gaussian potential: a dynamical system approach

Using a Dynamical Systems representation Morais *et al* PofDU [arxiv:1608.01679]; BL *et al*, JCAP [arXiv:1611.03100]

$$u = (\pi/2)\arctan(\chi/\chi_c) \qquad y = (\dot\chi + 3H\chi)/(3H\chi_c) \qquad z = \sqrt{\kappa^2 V/3H^2}$$

- Three **matter era** points:
  two repulsive - $(\pm 1, 0, 0)$
  one saddle - $(0, 0, 0)$
- One potential dom. **de Sitter** point: saddle - $(0, 0, 1)$
- Two **LSBR event** points:
  attractor - $(\pm 1/2, \pm 1, 0)$
- Four **unphysical** points:
  saddles - $(\pm 1, \pm 1, 0)$

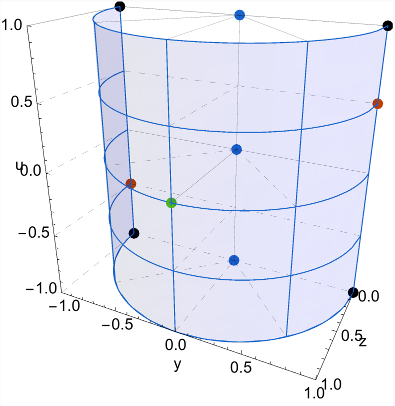

Fixed points in the non-interacting case

Fitting the model with a Gaussian potential-1-

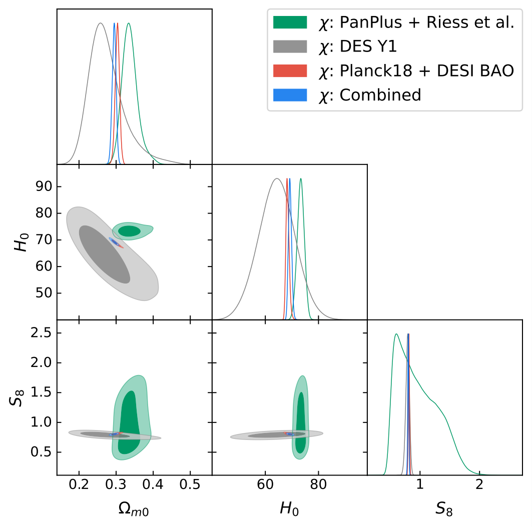

M.B.-L, H.-W. Chiang, C.G. Boiza, and P. Chen work in progress (2025)

Comparing the model to LCDM

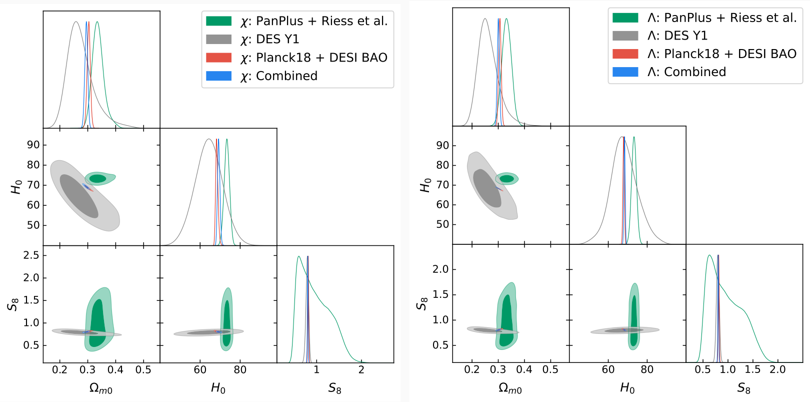

M.B.-L, H.-W. Chiang, C.G. Boiza, and P. Chen work in progress (2025)

Fitting the model with a Gaussian potential-2-

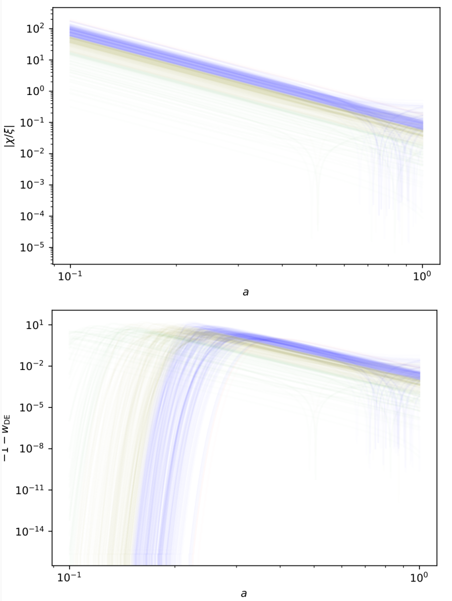

M.B.-L, H.-W. Chiang, C.G. Boiza, and P. Chen work in progress (2025)

Fitting the model with a Gaussian potential-3-

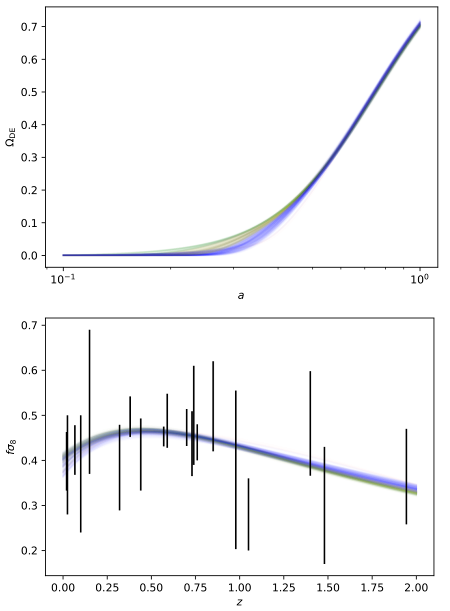

M.B.-L, H.-W. Chiang, C.G. Boiza, and P. Chen work in progress (2025)

Fitting the model with a Gaussian potential-4-

	CMB	+ BAO	+ SNe	+ low-z	+ DES Y1
$10^3\Omega_{b0}h^2$	22.20 ± 0.13	22.26 ± 0.13	22.24 ± 0.12	22.26 ± 0.13	22.30 ± 0.13
$10^3\Omega_{c0}h^2$	119.6 ± 1.1	118.79 ± 0.96	118.91 ± 0.87	118.9 ± 1.0	118.43 ± 0.99
$10^5\theta_{\rm MC}$	1040.79 ± 0.25	1040.88 ± 0.25	1040.88 ± 0.23	1040.88 ± 0.25	1040.93 ± 0.24
$\ln(10^{10}A_s)$	3.036 ± 0.014	3.041 ± 0.014	3.041 ± 0.014	3.039 ± 0.015	3.037 ± 0.015
n_s	0.9641 ± 0.0040	0.9662 ± 0.0037	0.9658 ± 0.0037	0.9660 ± 0.0039	0.9666 ± 0.0039
$\tau_{\rm reio}$	0.0520 ± 0.0071	0.0550 ± 0.0072	0.0549 ± 0.0074	0.0538 ± 0.0076	0.0537 ± 0.0078
$\log_{10}(\xi/M_P)$	1.6	1.6	1.7	1.7	1.7
$({\rm KE}_i + V_0)/\rho_{{\rm DE},0}$	1.0000 ± 0.0021	1.0002 ± 0.0027	1.0000 ± 0.0017	1.0004 ± 0.0020	1.0006 ± 0.0038
$\log_{10}(a_i^3\chi_i/\xi)$	$-2.3^{+0.6}$	$-1.6^{+0.3}$	$-1.86^{+0.69}_{-0.59}$	$-1.27^{+0.28}_{-0.21}$	$-1.23^{+0.27}_{-0.23}$
$(\dot\chi_i + 3H_i\chi_i)\rho^{-1/2}_{{\rm crit},h=1}$	0.00 ± 0.16	0.02 ± 0.17	0.00 ± 0.14	-0.01 ± 0.14	-0.04 ± 0.15
H_0	$67.57^{+0.58}_{-0.75}$	$68.29^{+0.56}_{-0.61}$	$68.02^{+0.45}_{-0.46}$	68.96 ± 0.59	69.18 ± 0.62
Ω_{m0}	$0.3116^{+0.0090}_{-0.0075}$	0.3030 ± 0.0059	0.3061 ± 0.0052	0.2983 ± 0.0052	0.2955 ± 0.0054
σ_8	$0.8076^{+0.0060}_{-0.0063}$	0.8079 ± 0.0070	0.8066 ± 0.0067	0.8109 ± 0.0067	0.8085 ± 0.0068
S_8	$0.822^{+0.013}_{-0.011}$	0.8118 ± 0.0096	0.8146 ± 0.0093	0.8085 ± 0.0086	0.8023 ± 0.0087
DIC	5498.76 ± 0.07	5507.33 ± 0.35	6209.97 ± 0.05	6215.61 ± 0.18	6475.8 ± 1.5
WAIC	5499.50 ± 0.09	5507.99 ± 0.03	6210.41 ± 0.19	6216.84 ± 0.19	6479.48 ± 0.43
$-\ln B$	5500.0 ± 1.2	5507.61 ± 0.02	6210.97 ± 0.47	6215.77 ± 0.17	6475.78 ± 0.18
ΔDIC	0.86 ± 0.16	0.12 ± 0.56	0.63 ± 0.18	-2.16 ± 0.54	-1.6 ± 1.5
ΔWAIC	0.41 ± 0.60	0.14 ± 0.22	0.05 ± 0.31	-1.84 ± 0.31	-1.68 ± 0.51
$-\Delta\ln B$	0.7 ± 1.8	-0.52 ± 0.86	0.46 ± 0.71	-3.4 ± 1.7	-4.1 ± 1.4

Table 4. Mean and standard deviation of cosmological parameters, late-time observables, and statistical probes for the 3-form dark energy model in section 2. From left to right are gradually larger datasets of CMB, CMB + BAO, CMB + BAO + SNe, etc., as defined in section 4.1. ΔICs are with respect to ΛCDM model presented in table 3. For parameters not following Gaussian distribution we provide the median and 68% lower and upper bounds (if valid) instead, with color coding for how heavy the tail is (red for short tail, black for Gaussian, blue for exponential, and cyan for long tail.) For single-sided distributions we report the modal and the single-sided 68% bound instead.

M.B.-L, H.-W. Chiang, C.G. Boiza, and P. Chen work in progress (2025)

Fitting the model with a Gaussian potential-5-

	BAO	SNe + low-z	DES Y1
$10^3\Omega_{c0}h^2$	116.7 ± 8.3	155 ± 11	86^{+23}_{-10}
$10^5\theta_{\rm MC}$	1042 ± 10	1090 ± 11	1005^{+45}_{-34}
$\ln(10^{10}A_s)$			$3.41^{+0.30}_{-0.26}$
H_0	68.71 ± 0.80	73.2 ± 1.3	65.9 ± 7.1
Ω_{m0}	0.295 ± 0.015	0.332 ± 0.018	$0.250^{+0.040}_{-0.032}$
σ_8			0.845 ± 0.086
S_8			0.791 ± 0.029
DIC	8.45 ± 0.05	703.37 ± 0.03	260.64 ± 0.75
WAIC	8.51 ± 0.15	703.31 ± 0.03	262.63 ± 0.10
$-\ln B$	8.86 ± 0.34	703.49 ± 0.11	262.35 ± 0.87
Tension against	CMB	CMB + BAO	CMB + BAO + SNe + low-z
$-\ln R$	0.0 ± 1.4	7.5 ± 1.6	-1.6 ± 2.1
GoF	$1.94 \pm 0.30\sigma$	$4.30 \pm 0.20\sigma$	$2.54 \pm 0.30\sigma$
S	$1.68 \pm 0.18\sigma$	$4.06 \pm 0.17\sigma$	$1.60 \pm 0.07\sigma$

Table 5. Mean and standard deviation of cosmological parameters, late-time observables, and statistical probes for ΛCDM model. From left to right are datasets of BAO, SNe + low-z, and DES Y1. Tension probes of $-\ln R$, GoF and S are with respect to ΛCDM model inside table 3 according to "Tension against" row. For parameters not following Gaussian distribution we provide the median and 68% lower and upper bounds (if valid) instead, with colour coding for how heavy the tail is (red for short tail, black for Gaussian, blue for exponential, and cyan for long tail.)

M.B.-L, H.-W. Chiang, C.G. Boiza, and P. Chen work in progress (2025)

Modified theory within $f(Q)$ gravity

Geometry of Spacetime: Metricity vs Non-Metricity

- We assume a space-time endowed with a metric $g_{\mu\nu}$ and a symmetric connection $\Gamma^{\lambda}_{\mu\nu}$, i.e. NO torsion:
- What is metricity, and how does it differ from non-metricity?

Metric Compatibility

$$\nabla_\lambda g_{\mu\nu} = 0$$

The covariant derivative of the metric tensor vanishes, meaning the length of vectors is preserved under parallel transport. Then the connection is uniquely determined by the metric and is given by the Levi-Civita connection.

Non-Metricity Tensor

$$Q_{\lambda\mu\nu} = \nabla_\lambda g_{\mu\nu} \neq 0$$

Represents the failure of the connection to preserve the metric under parallel transport. Therefore, the lenght of a vector may change.

J. M. Nester and H.-J. Yo, 1999

Curvature of Spacetime: Metricity vs Non-Metricity

- The scalar curvature of a space-time endowed with a metric $g_{\mu\nu}$ and a symmetric connection $\Gamma^{\lambda}_{\mu\nu}$ can be written as:

$$R(\Gamma) = \mathcal{R}(\{\}) + \mathrm{Q} + \text{surface terms},$$

where

$$Q := -\frac{1}{4} Q_{\alpha\mu\nu} Q^{\alpha\mu\nu} + \frac{1}{2} Q_{\alpha\mu\nu} Q^{\mu\alpha\nu} + \frac{1}{4} Q_{\alpha} Q^{\alpha} - \frac{1}{2} Q_{\alpha} \tilde{Q}^{\alpha}$$
$$Q_{\alpha} := Q_{\alpha\mu}{}^{\mu} \qquad \tilde{Q}_{\alpha} := Q_{\mu\alpha}{}^{\mu}\ .$$

- For a vanishing $R(\Gamma)$ a theory with Lagrangian density linear on $\mathcal{R}(\{\})$, is equivalent to a theory with Lagrangian density linear in Q.
- The former statment does not apply to $f(\mathcal{R}(\{\}))$ and $f(\mathrm{Q})$ because of the surface term.
- This gives rise to $f(\mathrm{Q})$ gravity as a new avenue of exploration, particularly from a phenomenological perspective, for example.

J. Beltrán Jiménez, L. Heisenberg, and T. S. Koivisto, arXiv:1803.10185

$f(Q)$ gravity

- The gravitational action:

$$S = \int d^4x\sqrt{-g}\,[f(Q) + \mathcal{L}_M]\,.$$

- The equations of motion are deduced by varying the action with respect to the metric and the connection.
- The energy momentum tensor for matter is conserved.

J. Beltrán Jiménez, L. Heisenberg, and T. S. Koivisto, arXiv:1803.10185 (proposer of the theories)

R. Lazkoz, F. S. N. Lobo, M. Ortiz-Baños, and V. Salzano, arXiv:1907.13219 (among the first cosmological fits)

FLRW cosmology in $f(\mathrm{Q})$ gravity

- The metric:

$$\mathrm{d}s^2 = -N(t)\mathrm{d}t^2 + a^2(t)\left[\mathrm{d}r^2 + r^2\left(\mathrm{d}\theta^2 + \sin^2\theta\mathrm{d}\phi^2\right)\right] ,$$

- The connection must be consistent with the symmetries of the FLRW metric; it should also be symmetric and satisfy the flatness condition, i.e. $R(\Gamma) = 0$.
- There are three possible connections that satisfy the above criteria, highlighting the richness of the theory.
- From now on, we shall adopt the simplest choice for the connection, maintaining the FLRW metric in its standard form.

F. D'Ambrosio, L. Heisenberg, and S. Kuhn, arXiv:2109.04209, I. Ayuso, M. B.-L., C.-Y. Chen, X. Y. Chew, K. Dialektopoulos, Y. C. Ong, arXiv:2506.03506

Suitable $f(\mathbb{Q})$ models for cosmology-1-

- Friedmann and Raychauduri equations:

$$6f_Q H^2 - \frac{1}{2}f = \rho_m \qquad \left(12H^2 f_{QQ} + f_Q\right)\dot{H} = -\frac{1}{2}(\rho_m + p_m)\,.$$

- The conservation equation:

$$\dot{\rho}_m + 3H(\rho_m + p_m) = 0.$$

- Three potential candidates:

$$\begin{aligned} f_1(Q) &= Q\exp\left(\lambda Q_0/Q\right), \\ f_2(Q) &= Q + Q_0\exp\left(-\lambda Q_0/Q\right), \\ f_3(Q) &= Q + \lambda Q_0[1-\exp\left(-Q_0/Q\right)]. \end{aligned}$$

- All these models give rise to late-time acceleration.
- The first model previously analysed in F. K. Anagnostopoulos, S. Basilakos and E. N.Saridakis, arXiv:2104.15123 [gr-qc].

C.G. Boiza, M. Petronikolou, M.B.-L. and E. N. Saridakis: arXiv:2505.18264

Suitable $f(\mathbb{Q})$ models for cosmology-2-

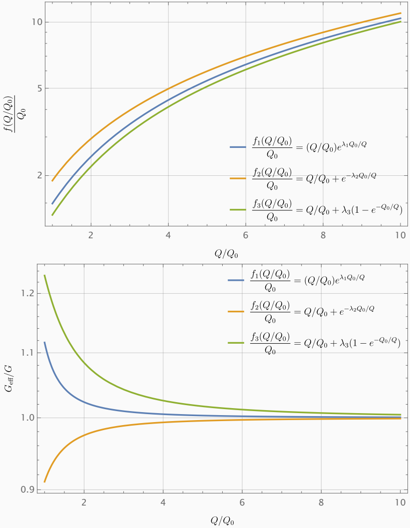

C.G. Boiza, M. Petronikolou, M.B.-L, E. N. Saridakis, arXiv:2505.18264

Observational constraints

- The analysis is performed for three different combinations of datasets:
  - **Combination I:** Cosmic chronometers (CC), supernovae (SN), and gamma-ray bursts (GRB);
  - **Combination II:** Baryon acoustic oscillations (BAO) and and redshift-space distortions (RSD);
  - **Combination III:** Full combination (CC + SN + GRB + BAO + RSD).

Fitting the model-1-

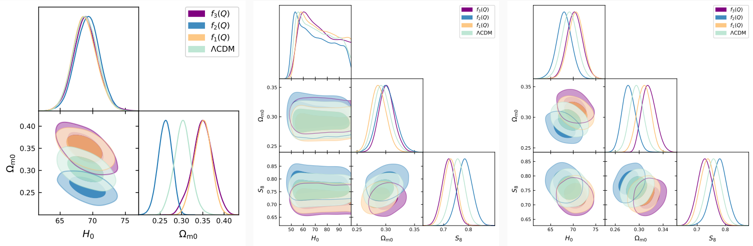

C.G. Boiza, M. Petronikolou, M.B.-L. and E. N. Saridakis: arXiv:2505.18264

Fitting the model-2-

Model	H_0	Ω_{m0}	r_d	S_8	ΔAIC
		CC + SN + GRB			
$f_3(Q)$	68.91 ± 1.90	0.3495 ± 0.0241	–	–	-0.23
$f_2(Q)$	69.20 ± 1.84	0.2616 ± 0.0160	–	–	1.67
$f_1(Q)$	68.76 ± 1.85	0.3497 ± 0.0200	–	–	0.17
ΛCDM	68.89 ± 1.86	0.3027 ± 0.0198	–	–	–
		BAO + RSD			
$f_3(Q)$	–	0.3015 ± 0.0133	–	0.7206 ± 0.0285	2.63
$f_2(Q)$	–	0.3013 ± 0.0156	–	0.7856 ± 0.0294	0.51
$f_1(Q)$	–	0.2877 ± 0.0132	–	0.7270 ± 0.0263	2.30
ΛCDM	–	0.2937 ± 0.0142	–	0.7567 ± 0.0279	–
		CC + SN + GRB + BAO + RSD			
$f_3(Q)$	70.31 ± 1.71	0.3163 ± 0.0117	147.09 ± 3.49	0.7280 ± 0.0270	6.08
$f_2(Q)$	68.01 ± 1.67	0.2827 ± 0.0109	147.62 ± 3.46	0.7773 ± 0.0280	5.19
$f_1(Q)$	70.56 ± 1.69	0.3080 ± 0.0113	146.98 ± 3.43	0.7361 ± 0.0264	8.90
ΛCDM	69.15 ± 1.73	0.2958 ± 0.0115	147.33 ± 3.57	0.7580 ± 0.0271	–

TABLE III: Mean values and standard deviations of the cosmological parameters obtained for each $f(Q)$ model, namely $f_1(Q) = Q\exp(\lambda Q_0/Q)$, $f_2(Q) = Q + Q_0\exp(-\lambda Q_0/Q)$, and $f_3(Q) = Q + \lambda Q_0[1 - \exp(-Q_0/Q)]$, and for ΛCDM paradigm, under the three different dataset combinations considered in this work: **Combination I** (CC + SN + GRB), **Combination II** (BAO + RSD), and **Combination III** (CC + SN + GRB + BAO + RSD). The parameter S_8 is derived from the fitted value of σ_8. The last column shows the AIC difference, $\Delta\text{AIC} \equiv \text{AIC}_{f(Q)} - \text{AIC}_{\Lambda\text{CDM}}$, quantifying the statistical preference relative to the ΛCDM model.

C.G. Boiza, M. Petronikolou, M.B.-L. and E. N. Saridakis: arXiv:2505.18264

Fitting the model-3-

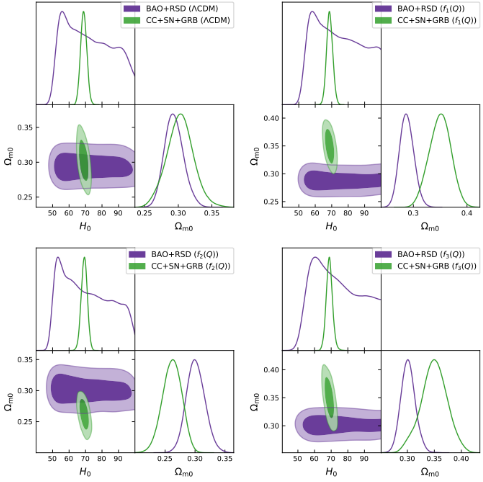

FIG. 3: *Comparison of the two-dimensional posterior distributions obtained from Combination I (CC + SN + GRB) and Combination II (BAO + RSD) for each model separately. The contours correspond to the 68% and 95% confidence levels (C.L.). The top-left panel shows the results for ΛCDM scenario, which displays excellent agreement between the two dataset combinations. The remaining panels correspond to Models 1 (top-right), 2 (bottom-left), and 3 (bottom-right), where a clear tension between the two combinations emerges in the $\Omega_{m0} - H_0$ plane. These internal inconsistencies contribute to the poorer global fits obtained by the $f(Q)$ models when all datasets are combined.*

Conclusions

Conclusions

- We have introduced a quitessence model that mimics a dynamical cosmological constant through a tracking regime, providing a fit as good as ΛCDM while also addressing the coincidence problem.
- We have described DE through a 3-form field with a Gaussian potential that can alleviate the H_0 tension.
- We have also discussed several $f(Q)$ models, highlighting the impact that $G_{\rm eff}$ can have on certain cosmological observables, and how useful these models can be in alleviating the H_0 and S_8 tensions.
- We are currently analysing certain extensions of the $\Lambda_{\rm s}$CDM model (O. Akarsu, S. Kumar, E. Özülker, J. A. Vázquez, arXiv:2108.09239), and the initial fits appear promising (in collaboration with B. Ibarra, arXiv:2506.12139, arXiv:2506.18992).

Thank you for your attention !!!

Theoretical model

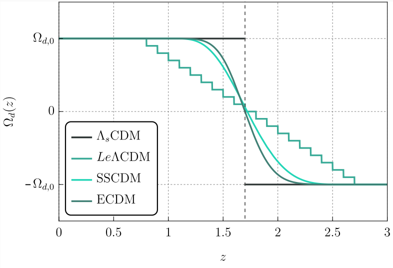

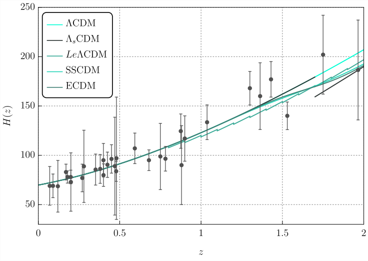

O. Akarsu, S. Kumar, E. Özülker, J. A. Vázquez, arXiv:2108.09239.

M.B.-L. and B. Ibarra-Uriondo arXiv: 2506.12139.

Cosmographic parameters

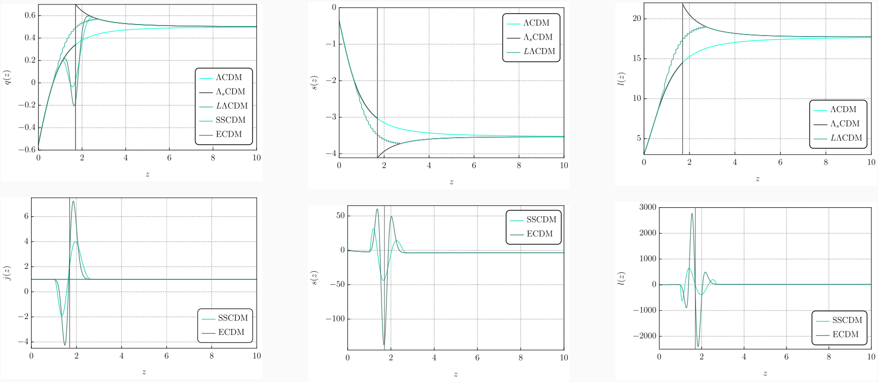

M.B.-L. and B. Ibarra-Uriondo arXiv: 2506.12139.

Gravitational potential

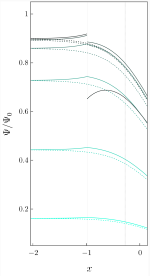

(A) Λ_sCDM

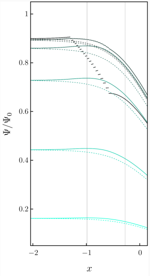

(B) LΛCDM

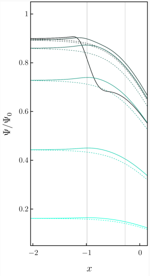

(C) SSCDM

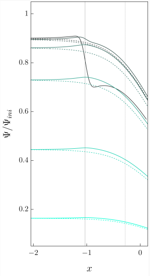

(D) ECDM

Gravitational potential Ψ/Ψ_{ini} for the four models compared with ΛCDM. Modes ranging between $\mathrm{k} = 3.33 \times 10^{-4}\mathrm{h\ Mpc}^{-1}$ and $\mathrm{k} = 0.1\mathrm{h\ Mpc}^{-1}$. We have set the initial conditions as $\Psi_{\rm ini} = 1$ (which implies $\delta_{\rm ini} = -2$), and subsequently rescale all resulting solutions by the physical value of $\delta_{\rm phys}(k)$.

M.B.-L. and B. Ibarra-Uriondo arXiv: 2506.18992.

fσ_8

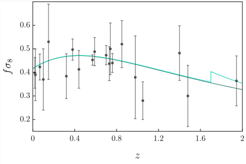

(A) Λ_sCDM

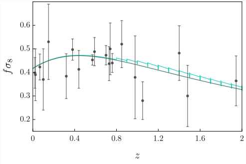

(B) LΛCDM

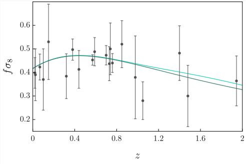

(C) SSCDM

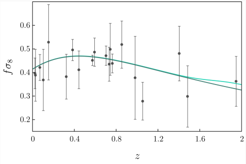

(D) ECDM

Evolution of $f\sigma_8$ for $0 < z < 2$. Light green lines: studied models. Dark green line: ΛCDM.

M.B.-L. and B. Ibarra-Uriondo arXiv: 2506.18992.